J_{AB} = 10.7 Hz, CH_AH_BOAc), 4.17 (1 H, B part of AB, J_{AB} = 10.7 Hz, CH_AH_BOAc), 5.8–6.0 (2 H, m, CH=CH); ^{13}C NMR ($CDCl_3$) δ 174.4, 170.9, 134.5, 134.3, 119.1, 85.4, 67.5, 51.7, 50.4, 48.6, 31.4, 30.2, 20.9, 17.4, 16.4; mass spectrum *m/e* 222.1136, calculated for $C_{12}H_{16}NO_3$ (M – CH_2OAc) = 222.1130; specific rotation ($CHCl_3$, *c* 1.1) $[\alpha]^{25}_D$ +84.2°.

Epoxide D13. A solution of 900 mg of 70% *tert*-butyl hydroperoxide in 50 mL of benzene was dried over 4-Å molecular sieves and added to 1.19 g (4.0 mmol) of the allylic alcohol D12, 10 mg of $VO(AcAc)_2$ was added, and the solution was stirred at 40 °C for 14 h. The crude reaction mixture was passed through a column of Florisil, eluting with hexane to remove excess hydroperoxide and then with CH_2Cl_2–EtOAc to afford the crude product. Recrystallization from CH_2Cl_2–hexane yielded 1.07 g (85%) of pure epoxide D13: mp (cor) 108.0–108.5 °C; IR ($CHCl_3$) 3020, 1735 cm^{-1}; ^1H NMR ($CDCl_3$, 200 MHz) δ 0.916 (3 H, s, CH_3), 1.7–2.7 (8 H, m), 2.143 (3 H, s, $OCOCH_3$), 3.583 (1 H, A part of AB, J_{AB} = 2.8 Hz, epoxide OCH), 3.648 (1 H, B part of AB, J_{AB} = 2.8 Hz, epoxide OCH), 3.677 (3 H, s, CO_2CO_3), 4.086 (1 H, A part of AB, J_{AB} = 11.8 Hz, CH_AH_BOAc), 4.294 (1 H, B part of AB, J_{AB} = 11.8 Hz, CH_AH_BOAc); ^{13}C NMR δ 174.7, 171.1, 118.7, 79.8, 79.6, 66.0, 62.5, 59.3, 51.5, 49.5, 43.6, 32.5, 29.5, 20.4, 15.7; mass spectrum *m/e* 238.1065, calculated for $C_{12}H_{16}NO_4$ (M – CH_2OAc) = 238.1079; specific rotation ($CHCl_3$, *c* 1) $[\alpha]^{25}_D$ 32.0°.

Epoxy Ketone D1. The hydroxy acetate D13 (470 mg, 1.5 mmol) in 20 mL of MeOH was treated with 200 mg of K_2CO_3 and 0.5 mL of H_2O. After 5 min, a solution of 400 mg of $NaIO_4$ in 5 mL of H_2O was added, followed after 16 h by another 100 mg of periodate. After 3 h, the methanol was evaporated, the aqueous solution was extracted with EtOAc, and the organic layer was washed with brine, dried ($MgSO_4$), and evaporated to afford 320 mg of an oil that was filtered through silica gel with CH_2Cl_2 to yield epoxy ketone D1 as an oil (220 mg, 65%): IR ($CHCl_3$) 3020, 2950, 1750 cm^{-1}; ^1H NMR ($CDCl_3$, 200 MHz) δ 1.05 (3 H, s, CH_3), 1.8–2.7 (7 H, m), 3.545 [1 H, A part of AB, J_{AB} = 2.2 Hz, COCH(O)CH], 3.66 (3 H, s, CO_2CH_3), 3.905 [1 H, B part of AB, J_{AB} = 2.2 Hz, COCH(O)CH]; ^{13}C NMR δ 209.5, 173.2, 117.6, 58.5, 55.4, 51.8, 47.5, 40.8, 35.7, 29.1, 17.5, 17.0; mass spectrum *m/e* 206.0815, calculated for $C_{11}H_{12}NO_3$(M – OCH_3) = 206.0817; Specific rotation $[\alpha]^{25}_D$ 9.4°.

Acknowledgment. The financial support of the National Science Foundation (NSF CHE75-09869 and CHE76-84340) is gratefully acknowledged. R.L. is grateful to the National Research Council of Canada for a fellowship. M.G.S. is grateful to the Swiss National Foundation for a fellowship, and R.S. and H.N.W. are grateful to the National Institutes of Health (NIH CA 06456 and NIH CA 06455, respectively) for a fellowship.

Electronic Structure of Ferricytochrome *c* and Associated Hyperfine Interactions†

K. C. Mishra, Santosh K. Mishra, and T. P. Das*

Contribution from the Department of Physics, State University of New York, Albany, New York 12222. *Received March 14, 1983*

Abstract: The electronic structure of ferricytochrome *c* has been investigated by the self-consistent charge extended Hückel procedure. By use of the spin distribution obtained from this calculation the hyperfine constants of ^{14}N and ^1H have been analyzed and found to provide satisfactory agreement with available electron nuclear double resonance data. The unpaired spin electron is found to be in a state involving a mixture of d_{XZ}- and d_{YZ}-like orbitals and the sulfur of the methionine group is found to carry a slight positive charge, in keeping with the postulates involved in the mechanism of electron transfer to and from cytochrome *c*.

In recent years, hyperfine interaction data for ^{14}N and ^1H nuclei have become available in ferricytochrome *c* through electron nuclear double resonance (ENDOR)[1] measurements.[2,3] It is therefore of interest to examine if one can explain these data through ab initio investigations of the electronic structures of this molecule, as has been possible in earlier work on other low- and high-spin heme systems.[4-6] The understanding of the electronic structure of ferricytochrome *c* is of particular interest because of the important role[7-9] it plays in electron transfer processes in a number of biological systems. In particular, in explaining the mechanism by which the ferricytochrome molecule gets reduced to the ferrous state, it has been proposed[10] that the unpaired spin orbital is in a π-like (d_{XZ} or d_{YZ}) state and that the sulfur of the methionine group carries a small positive charge that interacts electrostatically with the negative charge of an oxygen on the tyrosine molecule of the protein chain, this interaction providing a constraint on the orientation of the methionine group. It is therefore of interest to examine if these features ascribed to the ferricytochrome molecule are reproduced by ab initio investigations of its electronic structure.

Theoretical Procedures discusses briefly the structure of the model system used to represent ferricytochrome *c* in our investigations and the procedure for studying the electronic structure and hyperfine interactions. Results and Discussion presents and discusses the results for charge and spin distributions in the molecule and the ^{14}N and ^1H hyperfine interactions, making comparisons with available experimental data.[2,3] This comparison permits the assignment of the observed hyperfine constants to specific nitrogen and hydrogen atoms in the molecule.

Theoretical Procedures

Structure. The basic molecular unit that we have used to analyze the electronic structure and properties of low-spin fer-

† This work was supported by Research Grant HL15196 from the Heart, Lungs and Blood Institute of the National Institutes of Health.

(1) G. Feher, *Phys. Rev.*, **114**, 1219 (1959).
(2) C. P. Scholes and H. L. Van Camp, *Biochim. Biophys. Acta* **434**, 290 (1976).
(3) R. de Beer, personal communication.
(4) M. K. Mallick, S. K. Mun, S. L. Mishra, J. C. Chang, and T. P. Das, *J. Chem. Phys.*, **68**, 1642 (1978).
(5) S. K. Mun, J. C. Chang, and T. P. Das, *Biochim. Biophys. Acta*, **490**, 249 (1977); *J. Am. Chem. Soc.*, **101**, 5562 (1979).
(6) S. K. Mun, M. K. Mallick, S. L. Mishra, J. C. Chang, and T. P. Das, *J. Am. Chem. Soc.*, **103**, 5024 (1981).
(7) R. Lemberg and J. W. Legge, "Hematin Compounds and Bile Pigments", Interscience, New York, 1949.
(8) E. Margoliash and A. Schejter, *Adv. Protein Chem.*, **21**, 113 (1966).
(9) (a) E. Racker in "Membranes of Mitochondria and Chloroplasts", E. Racker, Ed., Van Nostrand Rheinhold, New York, 1970, pp 127. (b) S. Taniguchi, and M. D. Kamen, *Biochim. Biophys. Acta*, **96**, 395 (1965). (c) J. J. Hopfield, *Proc. Natl. Acad. Sci. U.S.A.*, **71**, 3640 (1974). (d) M. Y. Okamura and G. Feher, *Biophys. J.*, **41**, 122a (1983).
(10) F. R. Salemme, S. T. Freer, Ng. H. Xuong, R. A. Alden, and J. Kraut, *J. Biol. Chem.*, **248**, 3910 (1973).

0002-7863/83/1505-7729$01.50/0

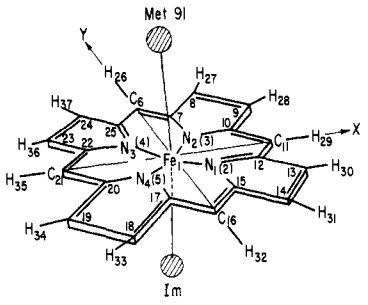

Figure 1. Ferricytochrome *c* molecule showing the atoms in the porphyrin base numbered according to the scheme in Table I. For the porphyrin nitrogen atoms, the numbers in the parentheses refer to the atom numbers in Table I and the suffixes to the usual notation in the literature. The imidazole and methionine ligands are displayed in detail in Figure 2.

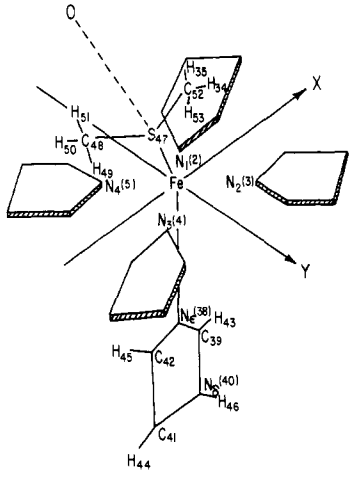

Figure 2. Ferricytochrome *c* showing methionine and imidazole ligands with atoms numbered according to the scheme in Table I. For the nitrogen atoms, the numbers in the parentheses have the same meaning as in Figure 1. The Fe–N_ϵ and Fe–S are 1.7 and 2.8 Å, respectively (ref 10, Table II).

ricytochrome *c* is shown in Figures 1 and 2. This unit was considered to be both representative of the heme unit (including fifth and sixth ligands) of the ferricytochrome *c* system and at the same time to have the maximum size that could be handled practically from a computational point of view. The porphyrin base was taken to have 4-fold symmetry with the side chains of the pyrrole rings being replaced by protons as in earlier work[4-6] on other heme systems. The plane of the protoporphyrin was chosen as the *XY* plane with *X* and *Y* axes passing respectively through the C_{11}, C_{21} and C_6, C_{16} mesocarbons. The positions of Fe and the fifth and sixth ligands as shown in Figure 2 were taken from X-ray data.[11] The fifth ligand is a protonated histidine, coplanar with the *XZ* plane. The sixth ligand is methionine (Met-91) with the Fe–S bond tilted away from the *Z* axis by 0.5 Å toward the N_4 atom of the protoporphyrin. For computatioal reasons it was not possible to include the entire Met-91 unit in our investigation. However, to understand the role of sulfur, the ligands of sulfur were chosen in the model so as to simulate its actual environment in ferricytochrome *c*. In accordance with observations in the X-ray analysis,[10] the lines joining sulfur to its four neighbors were considered to be tetrahedrally oriented. One of the four neighbors was Fe, a second was a methyl group, and the third was chosen to be another methyl group, replacing the chain CH_2–CH_2–CH–(NH_2)–COOH of Met-91. The fourth neighbor of sulfur, namely, the oxygen of tyrosine, was not included in the model system because of the large S–O separation[10] of 3.1 Å, which is substantially greater than the typical S–O covalent bond length of 1.47 Å. Because at such a large separation one does not expect any significant mixing of oxygen and sulfur wave functions, the exclusion of oxygen should not lead to any significant alteration of the electron distribution around S. However, as will be discussed later in the paper, the charge on the sulfur atom does have important significance[10] for its electrostatic interaction with the oxygen of tyrosine.

Calculation of Electronic Wave Functions. The electronic wave functions for ferricytochrome *c* were obtained by using the self-consistent extended Hückel procedure (SCCEH). The theory of the SCCEH procedure has been discussed in detail in the literature.[12] For the sake of completeness, however, we shall briefly describe certain features of this technique, which are crucial for understanding the results of our calculation.

In this method the molecular orbitals (MO) ψ_μ are expressed as linear combinations of atomic orbitals (AO) χ_i in the form

$$\psi_\mu = \sum_i C_{\mu i}\chi_i \tag{1}$$

where the coefficients $C_{\mu i}$ represent MO coefficients obtained by solving the equations

$$\sum_j C_{\mu i}(\mathcal{H}_{ij} - S_{ij}E_\mu) = 0 \tag{2}$$

$\mathcal{H}_{ij}$ and S_{ij} in eq 2 represent the Hamiltonian and overlap matrix elements. The Hamiltonian is constructed empirically from the ionization energies, ϵ_i and the charges q_l on atoms *l* obtained from the coefficients $C_{\mu i}$ by using the Mulliken approximation:

$$\begin{aligned} q_l &= -\sum_i^l (q_{li}^{\alpha} + q_{li}^{\beta}) + \zeta_l \\ q_{li}^{\alpha,\beta} &= \sum_\mu (|C_{\mu i}|^2 + \sum_{m\neq l}^{m}\sum_j C_{\mu i}C_{\mu j}S_{ij})n_\mu^{\alpha,\beta} \end{aligned} \tag{3}$$

where α and β represent spin states, $n_\mu^{\alpha,\beta}$ represents the populations of μth occupied orbital for the two different spin states, and ζ_l represents the valence charge on atom *l*. The q_l's are incorporated in $\mathcal{H}$ through the equations

$$\begin{aligned} \mathcal{H}_{ii} &= \epsilon_i^0 \pm |q_l|(\epsilon_i^{\pm} - \epsilon_i^0) \\ \mathcal{H}_{ij} &= \frac{K}{2}(\mathcal{H}_{ii} + \mathcal{H}_{jj})S_{ij} \end{aligned} \tag{4}$$

with ϵ_i^0, ϵ_i^+, and ϵ_i^- the ionization energies for the neutral atom, positive ion, and negative ions and *K* the Wolfsberg–Helmholtz parameter, usually taken as 1.89 for heme systems.[12] In the SCCEH method, self-consistency with respect to charge is usually achieved through the iterative procedure until the charge on each atom stabilizes within a chosen tolerance limit.

Calculation of Hyperfine Constants. The nuclear spin Hamiltonian, $\mathcal{H}_{spin}$, for an electronic system with spin $\vec{S}$ and a nucleus with spin $\vec{I}$ in the presence of a magnetic field along the *Z* direction is given by[13]

$$\begin{aligned} &\mathcal{H}_{spin} = \\ &\quad g_{ZZ}\mu_B HS_Z + A_{ZZ}I_ZS_Z + P_{ZZ}[I_Z^2 - I(I+1)] - \mu_N HI_Z \end{aligned} \tag{5}$$

where g_{ZZ}, A_{ZZ}, and P_{ZZ} represent the *ZZ* components respectively of the electronic *g* tensor and magnetic hyperfine and quadrupole coupling tensors, μ_B and μ_N representing the Bohr magneton and nuclear magnetic moment. The A_{ZZ} and P_{ZZ} in eq 5 can be obtained from the expectation value of the electron nuclear hyperfine interaction Hamiltonian, $\mathcal{H}_{eN}$, over the many-electron wave function,[14] with

(11) (a) R. E. Dickerson, T. Takano, D. Eisenberg, O. B. Kallai, L. Samson, A. Cooper, and E. Margoliash, *J. Biol. Chem.*, *246*, 1511 (1971). (b) Reference 10. (c) F. R. Salemme, J. Kraut, and M. D. Kamen, *J. Biol. Chem.*, *248*, 7701 (1973).

(12) (a) M. Zerner, M. Gouterman, and H. Kobayashi, *Theo. Chim. Acta*, 6, 363 (1966). (b) P. S. Han, T. P. Das, and M. F. Rettig, *Theo. Chim. Acta.*, 16, 1 (1970).

(13) Reference 2.

(14) T. P. Das in "Relativistic Quantum Mechanics of Electrons", Harper and Row, New York, 1973, p 184.

$$\mathcal{H}_{eN} = \frac{8\pi}{3}\gamma_e\gamma_N\hbar^2\vec{I}\sum_i\vec{S}_i\delta(\vec{r}_i) + \gamma_e\gamma_N\hbar^2\sum[3(\vec{S}_i\cdot\vec{r}_i)\times(\vec{I}\cdot\vec{r}_i) - r^2(\vec{I}\cdot\vec{S}_i)]/r_i^5 + \frac{e^2Q}{2I(I-1)}\left[\sum_N\frac{\zeta_N(3Z_N^2 - r_N^2)}{r_N^3}(3I_Z^2 - \vec{I}^2) - \sum_i(3I_Z^2 - \vec{I}^2)\frac{(3Z_i^2 - r_i^2)}{r^3}\right] \quad (6)$$

The first two terms in eq 6 correspond to the Fermi-contact and dipolar interactions and the third term is the quadrupole interaction for the nucleus with quadrupole moment Q; $\gamma_e = 2.0023$ and $\gamma_N = \mu_N/(I\hbar)$ refer to the gyromagnetic ratios for the electron and nuclear spins. The r_N in eq 6 refers to the distance of an electron from nucleus N and Z_N refers to the Z component of the radius vector $\vec{r}_N$. On taking the expectation value of $\mathcal{H}_{eN}$ and comparing it with eq 5, one obtains[4]

$$A_{ZZ} = A_F + B_{ZZ}$$

$$A_F = \frac{8\pi}{3}\left(\gamma_e\gamma_N\frac{\hbar^2}{2S}\right)\sum_\mu[|\psi_{\mu\uparrow}(o)|^2 - |\psi_{\mu\downarrow}(o)|^2]$$

$$B_{ZZ} = \gamma_e\gamma_N\frac{\hbar^2}{2S}\sum_\mu\left[\langle\psi_{\mu\uparrow}(\vec{r})\rangle - \left\langle\psi_{\mu\downarrow}(\vec{r})\left|\frac{3\cos^2\theta - 1}{r^3}\right|\psi_{\mu\downarrow}(\vec{r})\right\rangle\right]$$

$$P_{ZZ} = \frac{3}{4}\frac{e^2Q}{I(2I-1)}\left\{\sum_N\zeta_N\frac{3\cos^2\theta_N - 1}{r_N^3} - \left[\sum_\mu\left\langle\psi_{\mu\uparrow}(\vec{r})\left|\frac{3\cos^2\theta - 1}{r^3}\right|\psi_{\mu\uparrow}(\vec{r})\right\rangle + \left\langle\psi_{\mu\downarrow}(\vec{r})\left|\frac{3\cos^2\theta - 1}{r^3}\right|\psi_{\mu\downarrow}(\vec{r})\right\rangle\right]\right\} \quad (7)$$

with the summations over μ referring to the occupied orbitals. The parameters A_F and B_{ZZ} refer to isotropic and dipolar magnetic coupling constants, respectively. In eq 7, the spin orbitals $\psi_{\mu\uparrow}$ and $\psi_{\mu\downarrow}$ are in general different from each other because of exchange polarization (EP) of the paired orbitals by the valence electron with unpaired spin. This difference leads to a nonzero contribution to A_F and B_{ZZ} from the paired MO's. As will be seen in the next section, the EP effect for the protons can be as significant as the direct contributions arising from the unpaired spin orbital. This effect can be obtained by performing unrestricted Hartree-Fock[15] calculations with the different exchange interactions for up and down spin states properly included. Because the SCCEH procedure is essentially a restricted Hartree-Fock formalism, the EP effect is not included. One has therefore to consider the contributions to the magnetic hyperfine constants separately as we shall remark later in this section in discussing the procedures for treating the ^{14}N and ^1H hyperfine constants individually.

(1) Calculation of Magnetic Hyperfine Constants for ^{14}N. One can separate the contact term in eq 1 into two parts:

$$A_F = A_d + A_{ex} \quad (8)$$

where A_d and A_{ex} refer to direct and EP contributions as discussed in the previous section. For the ^{14}N nucleus, A_d will arise primarily from the χ_{2s} (the nitrogen 2s orbital) component of the unpaired molecular orbital, with very small contributions[16] from the tails of orbitals on neighboring atoms. If $C_{\mu 2s}$ is the molecular orbital coefficient of the unpaired MO, then using eq 7 one can write to a very good approximation

$$A_d = \frac{8\pi}{3}\gamma_e\gamma_N\hbar^2|C_{\mu 2s}|^2\chi_{2s}^2(o) \quad (9)$$

$\chi_{2s}^2(o)$ being the density due to the nitrogen atom Hartree-Fock 2s orbital at the ^{14}N nucleus. Since, as in earlier work[4-6] in heme systems, the unpaired spin orbital has significant nitrogen 2s character, A_d is expected to be the major contributor to A_F in eq 8. A quantitative evaluation of A_{ex} is difficult and semiempirical formulas[17] have been proposed for it in the literature when a nitrogen atom is bonded to carbon as in most nitrogen-containing free radicals with the unpaired electron in a π state. The major contribution to A_{ex} in these systems arises from the π spin density on the nitrogen atom and is positive in sign. The carbon atom unpaired spin populations lead to negative contributions that are relatively smaller than the nitrogen π spin-density contribution because the exchange interaction between paired orbitals on nitrogen and unpaired orbital components on carbon is weak. In the present situation, for the imidazole N_ϵ and the pyrrole nitrogens, one of the neighboring atoms is an iron atom that carries a substantial unpaired spin population (Table I) more than 15 times that on the nitrogen atom. One therefore expects sizable negative contribution from the spin population on the iron atom that could neutralize the positive contribution from the π-orbital spin population on nitrogen. In the absence of any quantitative information about this situation, we have made the reasonable assumption of complete cancellation between the two contributions and neglected A_{ex} for the pyrrole and imidazole N_ϵ nitrogens. For the imidazole N_δ nitrogen, the iron unpaired spin population is too far to contribute significantly and we shall make use of the empirical formula for A_{ex} for nitrogen bonded to carbon atoms. There is also an important contribution from the dipolar term B_{ZZ} to the net hyperfine constant A_{ZZ}, which further reduces the importance of A_{ex}. The direct contribution to B_{ZZ} from eq 7 leads to

$$B_{ZZ} = \gamma_e\gamma_N\hbar^2\left\langle\psi_\mu\left|\frac{3\cos^2\theta - 1}{r^3}\right|\psi_\mu\right\rangle \quad (10)$$

where ψ_μ in eq 10 refers to the single unpaired orbital in the present system. Because the MO ψ_μ is a linear combination of AO centered at different nuclei, a complete evaluation of the integral in eq 10 will involve one-, two-, and three-center integrals. In the case of ^{14}N, where there is significant nitrogen 2p character in the MO ψ_μ, the local one-center contribution will be much larger than the effect of other AO components. The local contribution to B_{ZZ} is given by the expression

$$B_{ZZ} = \gamma_e\gamma_N\hbar^2\langle r^{-3}\rangle_{2p}\left[\frac{2}{5}(2|C_{\mu Z}|^2 - |C_{\mu X}|^2 - |C_{\mu Y}|^2)\right] \quad (11)$$

where $C_{\mu Z}$, $C_{\mu X}$, and $C_{\mu Y}$ refer to the coefficients of the nitrogen $2p_Z$, $2p_X$ and $2p_Y$ orbitals in the unpaired MO and the value of $\langle r^{-3}\rangle$ was obtained from Hartree-Fock wave functions.[19] There can also be some EP contribution to B_{ZZ} from the unpaired spin orbitals. From atomic calculations,[18] such effects are expected to be rather small.

(2) Calculation of Magnetic Hyperfine Constants of ^1H. The unpaired MO in the present system has π-like symmetry about the CH bonds associated with the mesoprotons, the protons of the porphyrin system for which the ENDOR spectrum of the heme is usually studied.[20] The direct density at these protons due to the unpaired spin electron is therefore expected to vanish. Also, for the protons of the methionine and proximal imidazole ligands, the direct densities were found to be small. Therefore, unlike the case of ^{14}N, A_{ex} has relatively more importance and has to be included in the expression for A_F. To obtain A_{ex} we shall make

(15) R. E. Watson and A. J. Freeman in "Hyperfine Interactions" A. J. Freeman and R. B. Fraenkel, Eds., Academic Press, New York, 1971, p 53.
(16) Reference 12b.
(17) E. W. Stone and A. H. Maki, *J. Chem. Phys.*, **39**, 1635 (1963).
(18) R. M. Sternheimer, *Phys. Rev.*, **86**, 1 (1952). J. D. Lyons, R. T. Pu, and T. P. Das, *Phys. Rev.*, **178**, 103 (1969); **186**, 266 (1969).
(19) D. R. Hartree and W. Hartree, *Proc. R. Soc. London, Ser. A* **193**, 299 (1948). E. Clementi and C. Roetti in "Atomic Data and Nuclear Data Tables", Academic Press, New York, 1974.
(20) (a) C. P. Scholes, A. Lapidot, R. Mascarenhas, T. Inubushi, R. A. Isaacson, and G. Feher, *J. Am. Chem. Soc.*, **104**, 2724 (1982). (b) H. L. Van Camp, C. P. Scholes, and C. F. Mulks, *J. Am. Chem. Soc.*, **98**, 4094 (1976).

Table I. Charges and Unpaired Spin Populations on Various Atoms of Ferricytochrome

atom no.[a]	atom type	charge	unpaired spin population	atom no.[a]	atom type	charge	unpaired spin population
1	Fe	0.2390	0.6563	28	H	0.0606	0.0
2	N_1	−0.1720	0.0413	29	H	0.0860	0.0
3	N_2	−0.1790	0.0134	30	H	0.0609	0.0
4	N_3	−0.1803	0.0072	31	H	0.0612	0.0
5	N_4	−0.1734	0.0369	32	H	0.0857	0.0
6	C	−0.0188	0.0132	33	H	0.0618	0.0
7	C	0.0298	0.0003	34	H	0.0614	0.0
8	C	−0.0437	0.0047	35	H	0.0865	0.0
9	C	−0.0437	0.0016	36	H	0.0609	0.0
10	C	0.0330	0.0031	37	H	0.0610	0.0
11	C	−0.0157	0.0173	38	N_ϵ	−0.1058	0.0184
12	C	0.0309	0.0063	39	C	0.0714	0.0289
13	C	−0.0450	0.0018	40	N_δ	−0.0189	0.0254
14	C	−0.0444	0.0079	41	C	0.0125	0.0147
15	C	0.0285	0.0002	42	C	0.0060	0.0091
16	C	−0.0159	0.0246	43	H	0.1116	0.0001
17	C	0.0292	0.0014	44	H	0.0879	0.0
18	C	−0.0414	0.0132	45	H	0.0874	0.0
19	C	−0.0419	0.0065	46	H	0.0799	0.0
20	C	0.0319	0.0081	47	S	0.0273	0.0038
21	C	−0.0135	0.0196	48	C	−0.0946	0.0005
22	C	0.0350	0.0037	49	H	0.1014	0.0
23	C	−0.0431	0.0004	50	H	0.0707	0.0001
24	C	−0.0431	0.0035	51	H	0.0644	0.0
25	C	0.0325	0.0008	52	C	−0.0798	0.0003
26	H	0.0847	0.0	53	H	0.0769	0.0001
27	H	0.0606	0.0	54	H	0.0705	0.0
				55	H	0.0766	0.0001

[a] The numbers in this column are taken from Figures 1 and 2.

use of empirical formulas[6,21] for π and σ unpaired electrons in CH bonds available in the literature. Thus

$$A_{ex} = \frac{Q}{2S}\rho \tag{12}$$

where ρ represents the fractional population of the unpaired electron on the adjacent carbon atom, S is the spin of the system equal to $^1/_2$ in our present system, and Q has the values −70 MHz[21] and 63 MHz,[6] respectively, for π and σ unpaired electrons.

The dipolar contribution B_{ZZ} can be obtained by using eq 10, with γ_N referring to the proton gyromagnetic ratio and r and θ being taken with respect to the proton as the origin. Because the proton does not have any p electrons, there will be no local contribution, the contribution to B_{ZZ} arising primarily from AO components on other atoms in the molecule. In evaluating B_{ZZ} in such a case, one can use a dipolar approximation[6]

$$B_{ZZ} = \frac{\gamma_e\gamma_N\hbar^2}{2S}\sum_{B\neq A}\rho_B\frac{3Z_{AB}^2 - r_{AB}^2}{r_{AB}^5} \tag{13}$$

where A refers to the proton and B to a neighboring atom. This approximation has been found to be accurate for non-nearest neighbors, the contribution from the nearest-neighbor atom, like a carbon, being about 15% higher when one computes[6] the two-center integrals involved in eq 10 for this contribution. The dipolar approximation in eq 13 takes into account the fact that the unpaired spin population is delocalized and distributed over atoms other than iron. This delocalization effect was seen in earlier work[6] to lead to departures in the proton hyperfine field from the value one obtains assuming the entire unpaired spin population to be localized on iron alone.

(3) Evaluation of the Quadrupole Coupling Constant P_{ZZ}. The electronic part in the expression for P_{ZZ} for the ^{14}N nucleus in eq 7 is similar to that for the dipolar term B_{ZZ} except for the replacement of the minus sign inside the braces by a plus sign and the use of the quadrupole moment instead of gyromagnetic ratios. The electronic contribution arises primarily from the local term, the AO's on other atoms screening the valence charge contributions (eq 7) almost completely as will be seen under Results and Discussion, from the small effective charges obtained for the various atoms. Thus, the quadrupole coupling term P_{ZZ} is effectively given by

$$P_{ZZ} = -\frac{3}{4}\frac{e^2Q}{I(2I-1)}\sum_\mu n(\mu)\left(|C_{\mu z}|^2 - \frac{|C_{\mu x}|^2 + |C_{\mu Y}|^2}{2}\right)\frac{2}{5}\left\langle\frac{1}{r^3}\right\rangle \tag{14}$$

where the summation over μ extends over all occupied orbitals, $n(\mu)$ being equal to 2 for the paired states and unity for the unpaired state and $\langle 1/r^3\rangle$ being the expectation over the nitrogen 2p Hartree–Fock wave function as in the case of B_{ZZ}.

Results and Discussion

The results of our calculation will be described and discussed under three categories, the charge and spin distributions over the atoms, the ^{14}N magnetic and quadrupole hyperfine interactions, and the proton hyperfine interactions.

Charge and Spin Distributions over Atoms. The charges and unpaired spin populations on the various atoms are presented in Table I. Although the porphyrin ring was chosen to have 4-fold symmetry, the presence of the methionine and imidazole ligands destroys this symmetry and makes all the atoms inequivalent. Therefore, we have separately listed the charges and spins of the 55 atoms in Table I. The features of the overall charge distribution are very similar to other low-spin heme systems.[22] The Fe atom, like all other atoms, in ferricytochrome *c*, came out to be close to neutral, which indicates strong covalent binding with other atoms. Similar strong departures from ionic Fe^{3+} behavior of the iron atom for other high-[4-6] and low-spin systems[22] have been found in earlier work. It can be seen that the sulfur of Met-91 carries a small but significant positive charge. This is interesting in light of the model recently proposed[10] to explain the tilted Fe–S bond and its effect on the electron transfer process. It was proposed that the tilting of the Fe–S bond away from the line perpendicular to the porphyrin plane could be due to electrostatic interaction between a small positive charge on sulfur and a small negative

(21) H. M. McConnell, *J. Chem. Phys.* **24**, 764 (1956).

(22) (a) S. K. Mun, Jane C. Chang, and T. P. Das, *Proc. Natl. Acad. Sci. U.S.A.*, 76, 4842 (1979). (b) S. L. Mishra, Ph.D. Thesis, State University of New York at Albany, 1981 (unpublished).

Table II. Magnetic and Nuclear Quadrupole Hyperfine Constants (in MHz) for ^{14}N Nuclei in Cytochrome *c*

atom no.	A_F	B_{ZZ}	A_{ZZ}	P_{ZZ}
2 (N_1)	0.514	5.245	5.759	0.525
3 (N_2)	0.259	1.568	1.827	0.600
4 (N_3)	0.247	0.588	0.835	0.628
5 (N_4)	0.459	4.680	5.139	0.557
38 (N_ϵ)	0.160	−1.492	−1.332	0.109
40 (N_δ)	2.351[a]	−2.196	0.155	−0.566

[a] A_F for N_δ includes the exchange polarization contribution as explained in the text.

charge on the oxygen of tyrosine, the two atoms being too far from each other to have any appreciable covalent bonding. The small but finite positive charge that we have found on sulfur atom lends support to the proposed model[10] of electrostatic interaction between sulfur and oxygen atoms.

The distribution of spin density in Table I also indicates strong covalency of iron atom with its ligands, with the iron atom carrying only 65% of the total spin distribution, the rest being delocalized over the entire molecule. The sulfur atom in methionine carries very little spin density as compared to other ligands. This is a result of the fact that the unpaired MO involves a mixture of d_{XZ} and d_{YZ} orbitals on iron and the latter do not have significnat overlaps with the sulfur orbitals. From Table I one notices that there is a substantial difference in the unpaired spin populations on the pair of nitrogens N_1, N_4 of the porphyrin ring and the pair N_2, N_3. An asymmetry of this scale between porphyrin nitrogens has not been seen in other high- and low-spin heme systems investigated earlier.[4-6,22] A possible explanation of this asymmetry in cytochrome *c* may be given based on the nature of the methionine ligand and the orientations of its component groups. The sulfur in the methionine group has tetrahedral coordination, the orientations of the two prongs of the tetrahedral structure being fixed by the iron and the oxygen atom of tyrosine. This fixes the orientations of the two S–C bonds (Figure 2) in which one of the carbon atoms belongs to a methyl group and the other to the CH_2–CH_2–CH–(NH_2)–COOH group that has been replaced in our model system by another methyl group. The two methyl groups are preferentially closer to N_1 and N_4, and in addition to having covalent bonding with the π orbitals of these atoms, they also overlap significantly with the π-like d_{XZ} and d_{YZ} orbitals of iron. They are thus able to act as bridges to bring about stronger interaction between the nitrogen atoms N_1 and N_4 and d_{XZ} and d_{YZ} components of the unpaired spin orbital in the molecule as reflected by the greater spin densities on these atoms compared to those on N_2 and N_3. It is interesting that while the sulfur atom by virtue of its position does not itself conjugate strongly with the d_{XZ} and d_{YZ} orbitals of iron that constitute the iron components of the unpaired spin orbital, it is, however, able to strongly influence the spin-density distribution on the porphyrin atom through its two methyl ligands. In the next two subsections, the spin densities and unpaired state wave functions are utilized to derive the magnetic hyperfine constants of ^{14}N and ^1H by using eq 9 and 11–13, both the paired and the unpaired state wave functions being needed for obtaining the quadrupole coupling parameters P_{ZZ} for ^{14}N using eq 14.

^{14}N Hyperfine Interactions. The calculated values of A_F, B_{ZZ}, A_{ZZ}, and P_{ZZ} for ^{14}N are presented in Table II. The nuclear magnetic moment and quadrupole moment utilized in evaluating these quantities from eq 9, 11, and 14 are $\mu_N = \gamma_N \hbar = 0.40361$ nuclear magnetons and $Q_N = 0.01 \times 10^{-24}$ cm^2, respectively. Also, in evaluating B_{ZZ} from eq 11 we have used for γ_e a value appropriate for g_{ZZ} corresponding to the magnetic field applied in a direction perpendicular to the porphyrin plane, since it differs significantly[23] from the free-electron *g* value. For the contact interaction, however, the free-electron γ_e was utilized. This approximation was considered plausible, because the contact interaction involves the isotropic or *s* components of the wave functions at the nuclei while the dipolar hyperfine interaction involves the non-s components that also contribute to the *g* shift. The contact interaction A_F is seen from Table II to be in general a small fraction of the dipolar interaction B_{ZZ}, so that the effects on A_{ZZ} of the neglect of EP contributions to A_F is not expected to be significant. Further, the results in Table II show that the A_{ZZ} for N_1 and N_4 on the heme system are similar to each other and substantially different from those for N_2 and N_3. This was expected from the differences of the spin densities found for these pairs in Table I. The quadrupole interaction parameters P_{ZZ} are, however, quite similar for all four porphyrin nitrogens, since P_{ZZ} depends on the charge density due to both the paired and unpaired spin orbitals, the differences in charge density due to the unpaired spin orbitals being diluted by the densities due to the paired orbitals.

Currently available experimental data[2] do not permit a detailed comparison of the individual hyperfine parameters in Table II with experiment. However, we shall utilize our calculated hyperfine parameters to make assignments of the observed ENDOR spectra with the individual ^{14}N nuclei in the system. Before doing this, we would like to remark that our results in Table II are in good agreement with observed ^{14}N hyperfine parameters in protohemin mercaptide,[24] which is expected to be representative of cytochrome *c* in having a sulfur ligand. Additionally, since it has no nitrogen fifth and sixth ligands, the observed hyperfine parameters are definitely associated with porphyrin ^{14}N nuclei. In the mercaptide system, the observed ^{14}N hyperfine interaction parameters lead to $A_{ZZ} = 5.44$ MHz and $P_{ZZ} = 0.36$ MHz. The observed $|A_{ZZ}|$ compares very well with the calculated $|A_{ZZ}|$ in Table II for N_1 and N_4 atoms and the observed $|P_{ZZ}|$ is in reasonably good agreement with the calculated $|P_{ZZ}|$ for all four porphyrin nitrogens. No values of $|A_{ZZ}|$ corresponding to porphyrin N_2 and N_3 atoms have been reported as yet and it would be interesting to make comparisons, when they become available, with our calculated results, since one would expect the asymmetry between the N_1, N_4 and N_2, N_3 atom to be significantly different in cytochrome *c* and the mercaptide complex because of the special nature of the bonding between the groups in the methionine ligand and the porphyrin ring discussed earlier in this section.

For the imidazole nitrogens, in the case of $^{14}N_\epsilon$, the dipolar contribution is seen to be the dominant one, the sign of the latter being opposite to those for the porphyrin nirogens, as one would expect from geometrical considerations. For $^{14}N_\delta$, the contact contribution A_F is significantly larger than for $^{14}N_\epsilon$, due to the influence of exchange polarization effects, the strong cancellation between A_F and B_{ZZ} leading to a small net hyperfine interaction for $^{14}N_\delta$. For the field gradient, in addition to differences in the unpaired spin orbital contribution for the two nuclei, a significant difference was also obtained in the paired spin orbital contributions.

In making comparisons between our theoretical results and available ENDOR spectra, we note that for a spin 1 nucleus with magnetic and quadrupole hyperfine interactions in an external magnetic field *H*, the ENDOR spectrum from each nucleus consists of pairs of doublets with frequencies given by[2]

$$h\nu_{ENDOR} = \left|\frac{1}{2}|A_{ZZ}| \pm |P_{ZZ}| \pm \mu_N H\right| \qquad (15)$$

Using this relation, the ENDOR pairs of doublets expected for the four porphyrin ^{14}N and the imidazole $^{14}N_\epsilon$ and $^{14}N_\delta$ are listed in Table III. It is to be noted that within each doublet the separation of frequencies is $2\mu_N H$ and between corresponding members of each doublet, the frequency separation is $2|P_{ZZ}|$. These relationships are seen to be satisfied with all the doublets in Table III except the lower frequency doublets for N_2, N_3, and N_ϵ. For these the second frequencies on the list are negative because $^1/_2|A_{ZZ}| - |P_{ZZ}|$ is less than $\mu_N H$. However, since the sign of the frequency is not measured in ENDOR, one takes the absolute value as indicated in eq 15. The relationship between the doublets involving $2|P_{ZZ}|$ and $2\mu_N H$ is restored when one

(23) C. Mailer and C. P. S. Taylor, *Can. J. Biochem.* **50**, 1048 (1972).

(24) Reference 2.

Table III. Theoretical and Observed Zeeman Pair Frequencies for ^{14}N in Cytochrome *c*

atom no.	frequencies of Zeeman pairs, MHz		
	theoretical		observed
2 (N_1)	4.09	3.05	4.02 ± 0.01
	2.72	1.66	2.48 ± 0.08
5 (N_4)	3.82	2.70	2.70 ± 0.01
	2.44	1.32	1.40 ± 0.07
3 (N_2)	2.20	1.00	
	0.82	0.38	
4 (N_3)	1.74	0.48	
	0.36	0.90	
38 (N_ϵ)	1.47	1.25	
	0.09	0.13	
40 (N_δ)	1.41	0.28	
	0.03	1.10	

Table IV. Theoretical Proton Magnetic Hyperfine Constants (in MHz) Compared with Experimental ENDOR Results

atom no.[a]	A_F	B_{ZZ}	A_{ZZ}	experimental A_{ZZ}
26	−0.924	−1.254	−2.178	−2.24
29	−1.197	−1.455	−2.652	
32	−1.722	−1.775	−3.497	−5.18
35	−1.358	−1.586	−2.944	
43	−2.009	0.149	−1.86	−1.66
45	−0.642	0.569	−0.073	±0.20
46	−1.778	2.394	0.616	
49	0.0	0.458	0.458	
50	0.0	0.538	0.538	0.70
51	0.0	0.540	0.540	
53	0.0	1.063	1.063	1.20
54	0.0	0.870	0.870	

[a] The numbers in this column are taken from Figures 1 and 2. Protons 26–35 refer to mesoprotons, 34–46 to imidazole protons, and 49–54 to methionine protons.

recognizes that the three frequencies referred to earlier are absolute values of negative quantities.

In Table III we have also included the observed ENDOR frequencies.[2] A plausible assignment of the four observed frequencies that can fit the theoretical results in Table III would be to associate the observed pair 4.02 and 2.48 MHz with the first Zeeman pairs for N_1 and N_4 and to associate the other pair 2.70 and 1.40 MHz with the second Zeeman pairs of the same nuclei. This tentative assignment of the experimental Zeeman pairs leads to $|A_{ZZ}|_{expt}$ = 5.34 MHz and $|P_{ZZ}|_{expt}$ = 0.66 MHz. These are in very good agreement with the $|A_{ZZ}|$ and $|P_{ZZ}|$ for $^{14}N_1$ and $^{14}N_4$ nuclei on the porphyrin ring in Table II. One needs additional ENDOR lines to check the predicted doublet frequencies for the other ^{14}N nuclei in Table III. Additionally, selective ^{15}N ENDOR measurements would be of help in making assignments to compare with theory.

^1H Hyperfine Interactions. Following the procedure outlined under Calculation of Hyperfine Constants, we have used the electronic wave functions and spin populations on the various atoms to obtain the hyperfine fields at the proton sites corresponding to the mesoprotons and the proximal imidazole and methionine protons. The contributions from the contact and dipolar mechanisms are listed in Table IV. For the imidazole group, hydrogen atom 44 in Figure 2 has been substituted for a methyl group and does not represent a real hydrogen atom. Its hyperfine constant has therefore been dropped in Table IV. For the methionine ligand proton 55 in Figure 1 was really a replacement for the CH_2–C-H–(NH_2)–COOH group and did not represent a real proton. It has therefore also not been included in Table IV. We have included available experimental results for the proton hyperfine constants from ENDOR measurements,[3] where the signs were determined from Boltzmann factor dependent intensity considerations at the temperature of measurement, 1.5 K. Our results will be used to assign the observed hyperfine constants to individual protons in the system. In earlier work[6] on high-spin systems using the same procedure as employed in the present work, good agreement had been obtained between theory and measurements in cases where the latter had been experimentally assigned[20] to specific protons. Before proceeding to make assignments, we shall analyze the relative importance of different contributions to the total hyperfine constants A_{ZZ} for the various protons. Considering first the mesoprotons, both the dipolar and contact contributions are found to be comparable. The contact contribution arises from exchange polarization effects associated with the π orbitals on the carbon atom adjacent to the mesoprotons described by eq 12. The unpaired spin population on the adjacent carbon atoms also contributed significantly to the dipolar field at the mesoproton sites, and as in the case of the high spin systems,[6] it was important to include the contributions to the dipolar field from the unpaired populations from all the atoms in the molecule instead of using only that on the iron atom. The negative sign of the dipolar field is a consequence of the mesoproton lying on the porphyrin plane while the unpaired spin is directed along the direction of the applied field, which is perpendicular to the porphyrin plane.

For the imidazole protons, the dipolar contributions are positive and involve significant cancellations between positive and negative contributions from the unpaired spin populations on various atoms in the molecule. This cancellation effect leads to more significant differences between the dipolar contributions for the different imidazole protons as compared to those for the mesoprotons. The contact contributions that are negative again arise primarily from the π densities on adjacent carbon and nitrogen atoms and reflect the strengths of these densities. For the imidazole proton 43, the contact contribution dominates the dipolar and produces a sizable net negative A_{ZZ}, while for proton 45, the net A_{ZZ} is nearly zero from cancellation between A_{ZZ} and B_{ZZ}. For the proton 46 attached to N_δ, the dipolar contribution dominates over the contact and the net A_{ZZ} was positive. In this case, the dipolar term involved somewhat less cancellations of contributions from different atoms than in the case of the protons 43 and 45, the main contribution arising from the unpaired spin population on N_δ.

For the methionine protons the A_{ZZ}'s derived their entire value from B_{ZZ}, the dipolar contribution, since there is very little unpaired spin population on the adjacent carbon atoms of the methyl groups. Another consequence of this is that the dipolar contribution arises primarily from the iron atom with some small additional contributions from the nitrogen atoms N_1 and N_4 on the porphyrin plane, B_{ZZ} (eq 13), and hence A_{ZZ} being now positive as a consequence of the geometry of the proton.

As in the case of ^{14}N nuclei, we shall again attempt to assign the experimentally observed proton ENDOR spectra[3] to specific protons using the results of our calculation listed in Table IV. The observed hyperfine constant A_{ZZ} of largest magnitude is the one at −5.18 MHz as compared to the two largest ones from theory associated with mesoprotons H_{32} and H_{35}. The quantitative differences between these numbers and experiment are not serious, in view of the approximate eq 12 involved in obtaining the contact contributions and the approximate nature of the unpaired spin populations derived from SCCEH calculations. In the same spirit, one can assign the observed A_{ZZ} of −2.24 MHz to the porphyrin protons H_{26} and H_{29} and the observed A_{ZZ} of −1.66 MHz to the imidazole proton H_{43}. The imidazole proton H_{45} is seen from Table IV to have a value of A_{ZZ} close to zero due to cancellations between A_F and B_{ZZ} as remarked earlier and could be associated with the observed value of ±0.20. Because the hydrogen attached to N_δ is an exchangeable one, if the rate of exchange were fast enough, then one could not observe its hyperfine constant. If the rate of exchange is slow, then one would see it, but from Table IV, it appears that its ENDOR signal could merge with some of the methionine protons. Finally the two observed positive A_{ZZ}'s of 1.20 and 0.70 could be assigned to the methionine protons 53 and 54 and 49, 50, and 51, respectively.

In summary, the calculated results in Table IV lead to the following broad assignments of the observed proton hyperfine constants[3] from ENDOR measurements. The two largest negative A_{ZZ}'s appear to be associated with the mesoprotons on the porphyrin ring, the other negative and near zero A_{ZZ} with imidazole

protons, and the positive A_{ZZ} with protons in the methionine group.

Conclusion

The spin distribution obtained from SCCEH calculations for ferricytochrome *c* have provided a satisfactory explanation of observed ^{14}N and ^{1}H ENDOR data. The unpaired electron spin is found to be a π state involving admixture of d_{XZ} and d_{YZ}-like states and the sulfur of methionine is found to carry a small positive charge, in keeping with the proposition made in the literature in a qualitative description[10] of the mechanism of electron transfer to and from cytochrome. It is felt that the calculated electronic structure in this paper will be a useful starting point for further quantitative investigations of electron transfer between cytochrome *c* and donor or acceptor systems.

Acknowledgment. We are grateful to Professor C. P. Scholes and to Dr. R. de Beer from Technische Hogeschool Delft, The Netherlands for valuable discussions.

Registry No. Cytochrome *c*, 9007-43-6.

Antifungal Peroxide-Containing Acids from Two Caribbean Sponges†

Douglas W. Phillipson and Kenneth L. Rinehart, Jr.*

Contribution from the Roger Adams Laboratory, University of Illinois at Urbana-Champaign, Urbana, Illinois 61801. *Received March 23, 1983*

Abstract: Plakinic acids A and B, two new antifungal peroxy acids isolated from a Caribbean sponge, were assigned structures by spectroscopic techniques and by chemical degradation of their methyl esters, which were more easily purified. One of the acids contains the peroxide function as part of a five-membered ring. Plakortic acid, a carboxylic acid corresponding to plakortin, a previously described methyl ester, was isolated from another sponge. While the acids are potent antimicrobial compounds, the methyl esters, including plakortin, are essentially inactive.

A Caribbean sponge that grows like a shelf fungus in fairly deep water (at least down to 60 m) on rock or coral and has a smooth pink frosting-like outer layer over a fibrous charcoal-gray inner layer gave extracts among those most active from the Alpha Helix Caribbean Expedition[1] against *Saccharomyces cerevisiae* (a yeast) and *Penicillium atrovenetum* (a filamentous fungus) in a disk assay. The extracts also inhibited L1210 leukemia cells (ID_{50} 0.14 μg/mL). From samples of that sponge, collected by SCUBA, stored frozen or in isopropyl alcohol, and most recently identified as belonging to an apparently previously undescribed and still unnamed genus of the family Plakinidae,[2] we have isolated two peroxy acids that are responsible for the antifungal activity—plakinic acids A (**1**) and B (**2**), whose structure assignments we report here.

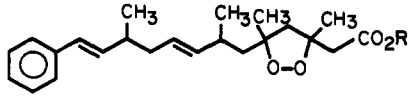

1 R = H

3 R = CH_3

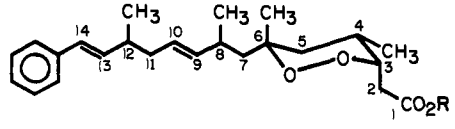

2: R = H

4: R = CH_3

The toluene phase from sponge samples extracted in the usual manner with 3:1 methanol–toluene[1] was applied to a reversed-phase medium-performance liquid chromatography (LC) column (Waters Associates C_{18} column packing from cracked Prep 500 cartridges, in Altex glass columns), gradient eluted in 10% steps from 70% methanol water through 100% methanol. Reversed-phase high-performance (HP)LC of bioactive fractions using 72.5% methanol–27.5% 0.01 N sodium acetate buffer (pH 4.6) yielded plakinic acids A and B (**1** and **2**), whose molecular formulas were established as $C_{23}H_{32}O_4$ and $C_{24}H_{34}O_4$, respectively, by high-resolution fast atom bombardment mass spectrometry (HRFABMS) employing xenon and glycerol[3] (417.2005, Δ 1.3 mmu, $M_A - H + Na_2$, $C_{23}H_{31}Na_2O_4$ requires 417.2018; 431.2138, Δ 3.7 mmu, $M_B - H + Na_2$, $C_{24}H_{33}Na_2O_4$ requires 431.2175).

The compounds were established as carboxylic acids by their IR spectra (**1**: broad band 3600–2600 cm^{-1}, carbonyl 1716 cm^{-1}) and by their conversion with diazomethane to the corresponding methyl esters **3** [$[\alpha]^{21}_D$ −57.8° (*c* 1.15)] and **4** [$[\alpha]^{21}_D$ −186.0° (*c* 5.00)] (carbonyl 1735 cm^{-1}), which could be easily separated by flash chromatography[4] on silica gel using 7% ethyl acetate in hexane (estimate of acids **1** and **2**: 0.01% and 0.1% in sponge). Crude methyl plakinate A (**3**) eluted first in the flash chromatography and was purified by HPLC on a semipreparative silica gel column with 2% ethyl acetate in hexane as the mobile phase.

The major skeletal fragment of **3** was assigned as unit a, $C_6H_5CH{=}CHCH(CH_3)CH_2CH{=}CHCH(CH_3)CHH-$, from extensive decoupling of its ^{1}H NMR spectrum [360 MHz; cf. supplementary material (see paragraph at end of paper regarding supplementary material)], with signals at δ 7.35–7.16 (m, 5 H), 6.33 (d, J = 16 Hz), 6.13 (dd, 16, 7.5 Hz), 2.36 (m), 1.07 (d, 3 H, 7 Hz), 2.1 (m, 2 H), 5.35 (m), 5.35 (m), 2.27 (m), 1.00 (d, 3 H, 7 Hz), 1.54 (dd, 14, 6 Hz), and 1.66 (dd, 14, 8 Hz) for the respective hydrogens and from its UV spectrum [$\lambda^{95\%EtOH}_{max}$ 246 nm

† This work was presented in part at the 186th National Meeting of the American Chemical Society, Washington, DC, Aug 28–Sept 2, 1983.

(1) Rinehart, K. L., Jr.; Shaw, P. D.; Shield, L. S.; Gloer, J. B.; Harbour, G. C.; Koker, M. E. S.; Samain, D.; Schwartz, R. E.; Tymiak, A. A.; Weller, D. L.; Carter, G. T.; Munro, M. H. G.; Hughes, R. G., Jr.; Renis, H. E.; Swynenberg, E. B.; Stringfellow, D. A.; Vavra, J. J.; Coats, J. H.; Zurenko, G. E.; Kuentzel, S. L.; Li, L. H.; Bakus, G. J.; Brusca, R. C.; Craft, L. L.; Young, D. N.; Connor, J. L. *Pure Appl. Chem.* **1981**, *53*, 795–817.

(2) Identification by Dr. G. J. Bakus, Department of Biological Sciences, University of Southern California, Los Angeles, CA 90089

(3) Rinehart, K. L., Jr. *Science* (*Washington*, D.C.) **1982**, *218*, 254–260.

(4) Still, W. C.; Kahn, M.; Mitra, A. *J. Org. Chem.* **1978**, *43*, 2923–2925.

0002-7863/83/1505-7735$01.50/0